in Proc. IEEE VTC1999/Fall
Amsterdam, The Netherlands, pp. 1465–1470, Sep. 1999

BOUNDS ON THE SYSTEMATIC MEASUREMENT ERRORS OF CHANNEL SOUNDERS FOR TIME-VARYING MOBILE RADIO CHANNELS*

Gerald Matz[a], *Andreas F. Molisch*[a,b], *Martin Steinbauer*[a], *Franz Hlawatsch*[a], *Ingo Gaspard*[c], *and Harold Artés*[a]

[a]Institute of Communications and Radio-Frequency Engineering, Vienna University of Technology
[b]FTW Forschungszentrum Telekommunikation Wien
[c]Deutsche Telekom AG, Technologiezentrum Darmstadt

ABSTRACT

We show that correlative sounders for time-varying mobile radio channels are affected by various systematic measurement errors. We identify and analyze these errors and provide quantitative error bounds in terms of channel and sounder parameters. Furthermore, we propose a novel calibration method yielding substantially improved accuracy. Experiments using measured data and computer simulations illustrate our theoretical results. Our findings allow to assess the accuracy of existing measurements as well as to devise improved measurement techniques.

1 INTRODUCTION

Accurate wideband measurements of mobile radio channels by means of wideband channel sounders are the cornerstone of any design or simulation of mobile radio systems with high data rate. Most of the popular channel sounders use correlative pulse compression techniques [1–3]. These techniques are usually based on the assumption that the channel is quasi-time-invariant (quasi-static), i.e., effectively constant during one sounding period. However, the recent use of higher carrier frequencies has resulted in larger Doppler shifts and, hence, faster time variations of the channel. These time variations cause systematic measurement errors that will be analyzed and quantified in the present paper. In addition, we propose a novel calibration method for fast time-varying channels.

The paper is organized as follows. Section 2 discusses basic channel descriptions and Section 3 describes some popular channel sounding techniques. In Sections 4 and 5, we investigate the errors affecting uncalibrated and calibrated measurements, respectively, and we present a novel calibration method. Finally, Section 6 provides simulation and measurement results.

2 MOBILE RADIO CHANNELS

A time-varying linear channel $\mathbf{H}$ can be characterized by its kernel $k_{\mathbf{H}}(t,t')$ which relates input and output as[1]

$$y(t) = (\mathbf{H}x)(t) = \int_{t'} k_{\mathbf{H}}(t,t')\, x(t')\, dt'.$$

The *impulse response* or *input delay spread function* is defined as $h^I_{\mathbf{H}}(t,\tau) \triangleq k_{\mathbf{H}}(t,t-\tau)$, and the *output delay spread function* is defined as $h^O_{\mathbf{H}}(t,\tau) \triangleq k_{\mathbf{H}}(t+\tau,t)$ [4]. We note the relation

$$h^I_{\mathbf{H}}(t,\tau) = h^O_{\mathbf{H}}(t-\tau,\tau). \qquad (1)$$

*Funding by EU project METAMORP (SMT4-CT96-2093) and FWF grants P11904-TEC and P12228-TEC.

[1]Unless stated otherwise, all integrals and sums go from $-\infty$ to ∞.

The Fourier transform of $h^I_{\mathbf{H}}(t,\tau)$ with respect to τ,

$$L^I_{\mathbf{H}}(t,f) \triangleq \mathop{\mathcal{F}}_{\tau\to f}\{h^I_{\mathbf{H}}(t,\tau)\} = \int_\tau h^I_{\mathbf{H}}(t,\tau)\, e^{-j2\pi f\tau}\, d\tau, \qquad (2)$$

is called *time-varying frequency response* [4]. Similarly, $L^O_{\mathbf{H}}(t,f) \triangleq \mathcal{F}_{\tau\to f}\{h^O_{\mathbf{H}}(t,\tau)\}$ is called *frequency-dependent modulation function* [4]. $L^I_{\mathbf{H}}(t,f)$ and $L^O_{\mathbf{H}}(t,f)$ are special cases of the *generalized Weyl symbol* [5]. The Fourier transforms of $h^I_{\mathbf{H}}(t,\tau)$ and $h^O_{\mathbf{H}}(t,\tau)$ with respect to t,

$$S^I_{\mathbf{H}}(\tau,\nu) \triangleq \mathop{\mathcal{F}}_{t\to\nu}\{h^I_{\mathbf{H}}(t,\tau)\}, \quad S^O_{\mathbf{H}}(\tau,\nu) \triangleq \mathop{\mathcal{F}}_{t\to\nu}\{h^O_{\mathbf{H}}(t,\tau)\}, \qquad (3)$$

are called *(delay-Doppler and Doppler-delay) spreading functions* [4]. They globally describe the delays (time shifts) τ and Doppler (frequency) shifts ν introduced by the channel. $S^I_{\mathbf{H}}(\tau,\nu)$ and $S^O_{\mathbf{H}}(\tau,\nu)$ are special cases of the *generalized spreading function* [5], and they are related as

$$S^I_{\mathbf{H}}(\tau,\nu) = S^O_{\mathbf{H}}(\tau,\nu)\, e^{-j2\pi\tau\nu}. \qquad (4)$$

Hereafter, we write $|S_{\mathbf{H}}(\tau,\nu)| = |S^I_{\mathbf{H}}(\tau,\nu)| = |S^O_{\mathbf{H}}(\tau,\nu)|$.

Underspread channels (or targets, in a radar context) are usually defined via a constraint on the support of the spreading function such that the product of maximum excess delay $\tau_{\max}$ and maximum Doppler shift $\nu_{\max}$ is less than one [6–8]. An alternative concept of underspread channels requires certain moments of the spreading function to be small [9]. The specific moments that will be relevant to our discussion are the *mean delays*[2]

$$\overline{\tau}^{(1)}_{\mathbf{H}} \triangleq \frac{1}{\|S_{\mathbf{H}}\|_1}\int_\tau\int_\nu |\tau|\,|S_{\mathbf{H}}(\tau,\nu)|\, d\tau\, d\nu,$$

$$\overline{\tau}^{(2)}_{\mathbf{H}} \triangleq \frac{1}{\|S_{\mathbf{H}}\|_2}\left[\int_\tau\int_\nu \tau^2\,|S_{\mathbf{H}}(\tau,\nu)|^2\, d\tau\, d\nu\right]^{1/2},$$

the *mean Doppler shifts* $\overline{\nu}^{(1)}_{\mathbf{H}}$ and $\overline{\nu}^{(2)}_{\mathbf{H}}$ (defined analogously), and the *mean delay-Doppler products*

$$\overline{\mu}^{(1)}_{\mathbf{H}} \triangleq \frac{1}{\|S_{\mathbf{H}}\|_1}\int_\tau\int_\nu |\tau\nu|\,|S_{\mathbf{H}}(\tau,\nu)|\, d\tau\, d\nu,$$

$$\overline{\mu}^{(2)}_{\mathbf{H}} \triangleq \frac{1}{\|S_{\mathbf{H}}\|_2}\left[\int_\tau\int_\nu (\tau\nu)^2\,|S_{\mathbf{H}}(\tau,\nu)|^2\, d\tau\, d\nu\right]^{1/2}.$$

In practical situations, these channel parameters can be determined from physical considerations or estimated from measurements with sufficient accuracy.

[2]The L_1 and L_2 norms of the spreading function are defined as $\|S_{\mathbf{H}}\|_1 \triangleq \int_\tau\int_\nu |S_{\mathbf{H}}(\tau,\nu)|\, d\tau\, d\nu$ and $\|S_{\mathbf{H}}\|_2 \triangleq \left[\int_\tau\int_\nu |S_{\mathbf{H}}(\tau,\nu)|^2\, d\tau\, d\nu\right]^{1/2}$, respectively.

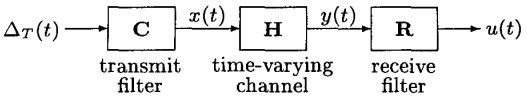

Figure 1. *Generic channel sounder model.*

3 CORRELATIVE SOUNDING METHODS

We shall now give a description of several popular sounding methods within a unified framework. This will provide a basis for analyzing the systematic measurement errors of these methods in Sections 4 and 5. In contrast to previous discussions [1–3], our description does not assume the channel to be quasi-time-invariant.

3.1 Idealized Channel Sounder

An idealized channel sounder [10] uses an impulse train $\Delta_T(t) = \sum_m \delta(t - mT)$ as sounding signal. The resulting channel output consists of "slices" of $k_{\mathbf{H}}(t, t')$,

$$y(t) = \int_{t'} k_{\mathbf{H}}(t, t')\, \Delta_T(t')\, dt' = \sum_m k_{\mathbf{H}}(t, mT)\,.$$

This idealized channel sounder can be viewed as a special case of the generic channel sounder model shown in Fig. 1, with transmit and receive filters $\mathbf{C} = \mathbf{R} = \mathbf{I}$ (with $\mathbf{I}$ the identity operator) such that $x(t) = \Delta_T(t)$ and $u(t) = y(t)$. For $\tau_{\max} \leq T$, the mth block of the output signal equals the output delay spread function[3] at time $t = mT$,

$$h^O_{\mathbf{H}}(mT, \tau) = u(\tau + mT)\, w(\tau)\,, \qquad (5)$$

where $w(t)$ denotes a rectangular window of duration T. Under certain conditions [10], the complete output delay spread function can be recovered by interpolating between successive measurements,

$$h^O_{\mathbf{H}}(t, \tau) = \sum_m h^O_{\mathbf{H}}(mT, \tau)\, \mathrm{sinc}\Big(\frac{\pi}{T}(t - mT)\Big)\,, \qquad (6)$$

with $\mathrm{sinc}(t) = \sin(t)/t$. Combining (5) and (6), we can write

$$h^O_{\mathbf{H}}(t, \tau) = (\Upsilon u)(t, \tau) = (\Upsilon \mathbf{H} \Delta_T)(t, \tau)\,, \qquad (7)$$

where Υ denotes the mapping of the output signal $u(t)$ to the measured output delay spread function $h^O_{\mathbf{H}}(t, \tau)$.

3.2 Generic Channel Sounder Model

The idealized sounder is impractical due to the large crest factor of the impulse-train sounding signal $\Delta_T(t)$. It has thus become common to use correlative pulse compression techniques. According to the generic channel sounder model depicted in Fig. 1, the sounding signal is

$$x(t) = (\Delta_T * c)(t) = \sum_m c(t - mT)\,,$$

where $c(t)$ is the impulse response of the time-invariant transmit filter $\mathbf{C}$ and $*$ denotes convolution. At the receiver front end, the channel output $y(t) = (\mathbf{H}x)(t)$ is passed through a time-invariant receive filter $\mathbf{R}$ with impulse response $r(t)$, which results in the signal $u(t) = (y * r)(t) = (\mathbf{RHC}\Delta_T)(t)$. This can be viewed as idealized sounding of the composite channel $\mathbf{RHC}$. From $u(t)$, an estimate of the output delay spread function at $t = mT$ can be calculated according to (5), i.e.,

$$\hat{h}^O_{\mathbf{H}}(mT, \tau) = u(\tau + mT)\, w(\tau)\,, \qquad (8)$$

[3]However, usually the output signal is erroneously interpreted as an estimate of $h^I_{\mathbf{H}}(mT, \tau)$, see Section 4.

and an estimate of the channel's frequency-dependent modulation function can be derived from $\hat{h}^O_{\mathbf{H}}(mT, \tau)$ as

$$\hat{L}^O_{\mathbf{H}}(mT, f) = \underset{\tau \to f}{\mathcal{F}} \big\{ \hat{h}^O_{\mathbf{H}}(mT, \tau) \big\}\,. \qquad (9)$$

In view of (8), this amounts to a Fourier transform of the mth block of $u(t)$. Estimates of $h^O_{\mathbf{H}}(t, \tau)$ and $L^O_{\mathbf{H}}(t, f)$ for $t \neq mT$ can then be obtained via interpolation (cf. (6)). In particular, we can write (cf. (7))

$$\hat{h}^O_{\mathbf{H}}(t, \tau) = (\Upsilon u)(t, \tau) = (\Upsilon \mathbf{RHC}\Delta_T)(t, \tau)\,. \qquad (10)$$

For proper operation of the correlative channel sounder outlined above, the impulse responses $c(t)$ and $r(t)$ of the transmit and receive filter, respectively, must be designed to satisfy $(c * r)(t) \approx \delta(t)$ (i.e., $\mathbf{RC} \approx \mathbf{I}$). If the channel $\mathbf{H}$ is time-invariant (static), then $\mathbf{H}$ and $\mathbf{R}$ commute, i.e., $\mathbf{RH} = \mathbf{HR}$, and the output signal becomes

$$u(t) = (\mathbf{RHC}\Delta_T)(t) = (\mathbf{HRC}\Delta_T)(t) = (\mathbf{H}\tilde{\Delta}_T)(t)\,,$$

with the *virtual sounding signal*

$$\tilde{\Delta}_T(t) \triangleq (\mathbf{RC}\Delta_T)(t) = \sum_m (c * r)(t - mT)$$

that approximates $\Delta_T(t) = \sum_m \delta(t - mT)$. This allows to *effectively* use an ideal impulse-train sounding signal without the drawback of a high crest factor. Unfortunately, a time-varying channel $\mathbf{H}$ commutes with the receive filter $\mathbf{R}$ only approximately at best (see Section 4).

Next, we discuss the three most common channel sounders as special cases of our general framework.

Correlation Sounder. Apart from the idealized sounder in Subsection 3.1, all sounders considered in this paper are correlative sounders. However, what is usually known as a *correlation sounder* is a sounder that uses a transmit pulse of the form

$$c(t) = \sum_{i=1}^{N} b_i\, p(t - iT_c)$$

and a matched receive filter $r(t) = c(T - t)$. Here, T_c is the chip length, $p(t)$ is the (typically rectangular) chip pulse, and b_i is a binary sequence. If b_i is a pseudonoise (PN) sequence, $(c * r)(t)$ is a reasonable approximation to a Dirac impulse. Variants of correlation sounders using sounding sequences other than PN sequences [11] or mismatched receive filters [12] still fit into our generic sounder model.

Swept Time-Delay Cross-Correlator (STDCC). While the correlation sounder described above requires a sampling rate of $1/\Delta\tau$ to obtain a delay resolution of $\Delta\tau$, the STDCC [13] obtains the same resolution with a sampling rate of only $1/(K\Delta\tau)$ where typically $K \approx 1000$. In practical implementations, the receiver uses a dilated version of the transmit PN sequence such that the receive filter length T_R is larger by $\Delta\tau$ than the transmit filter length T_T, i.e., $T_R = T_T + \Delta\tau$. It can be shown that an estimate of $h^O_{\mathbf{H}}(t, \tau)$ at time $t = mT_T$ and delay $\tau = (m \bmod K)\Delta\tau$ with $K = T_T/\Delta\tau$ is given by $u(mT_R)$,

$$\hat{h}^O_{\mathbf{H}}\big(mT_T, (m \bmod K)\Delta\tau\big) = u(mT_R)\,. \qquad (11)$$

It follows that successive measurements at the same delay are separated by $T_{\mathrm{rep}} = KT_R = 1/f_{\mathrm{slip}}$ where f_{slip} is called the *slip rate*. Since $T_{\mathrm{rep}} \gg T_T$, the STDCC is more sensitive to channel time variations than the conventional PN sounder (see Section 4).

Chirp Sounder. The chirp sounder [14] uses a chirp transmit pulse

$$c(t) = c_0\, e^{j2\pi t(f_L + \frac{a}{2}t)}, \quad 0 < t < T,$$

and receive filter $r(t) = c(T-t)$. The frequency range covered by the transmit pulse $c(t)$ is approximately $[f_L, f_L + aT]$. For sufficiently high bandwidth aT, $(c*r)(t)$ is a reasonable approximation to a Dirac impulse. Improvements can be obtained using nonrectangular (e.g., Gaussian) envelopes for $c(t)$ and $r(t)$ [15].

4 ANALYSIS OF MEASUREMENT ERRORS

For time-varying channels, the correlative sounding techniques described above are affected by systematic errors. The difference (error) between the measured output delay spread function $\hat{h}^O_{\mathbf{H}}(t,\tau) = (\Upsilon u)(t,\tau) = (\Upsilon\mathbf{RHC}\Delta_T)(t,\tau)$ in (10) and the true (desired) impulse response $h^I_{\mathbf{H}}(t,\tau)$ can be split into four components,

$$\hat{h}^O_{\mathbf{H}}(t,\tau) - h^I_{\mathbf{H}}(t,\tau) = \sum_{i=1}^{4} e_i(t,\tau),$$

which can be interpreted and expressed as follows:

- The "wrong order" of channel $\mathbf{H}$ and receive filter $\mathbf{R}$ (recall that correlative sounding assumes the systems to be ordered as $\mathbf{HRC}$ but in fact we have $\mathbf{RHC}$) causes a *commutation error*

$$\begin{aligned} e_1(t,\tau) &\triangleq \hat{h}^O_{\mathbf{H}}(t,\tau) - (\Upsilon\mathbf{HRC}\Delta_T)(t,\tau) \\ &= (\Upsilon\mathbf{RHC}\Delta_T)(t,\tau) - (\Upsilon\mathbf{HRC}\Delta_T)(t,\tau). \end{aligned} \tag{12}$$

- The transmit and receive filters do not yield perfect pulse compression, i.e., $(c*r)(t) \neq \delta(t)$ or $\mathbf{RC} \neq \mathbf{I}$. This leads to a *pulse compression error*

$$e_2(t,\tau) \triangleq (\Upsilon\mathbf{HRC}\Delta_T)(t,\tau) - (\Upsilon\mathbf{H}\Delta_T)(t,\tau). \tag{13}$$

  We note that the pulse compression error can be reduced by calibration (see Section 5).

- For channels with delays larger than T and/or Doppler shifts larger than[4] $1/(2KT)$, there occurs aliasing in the delay and/or Doppler domain. The resulting *aliasing error* is given by

$$e_3(t,\tau) \triangleq (\Upsilon\mathbf{H}\Delta_T)(t,\tau) - h^O_{\mathbf{H}}(t,\tau). \tag{14}$$

- Finally, the measured function $\hat{h}^O_{\mathbf{H}}(t,\tau) = (\Upsilon u)(t,\tau)$ is often erroneously used as an estimate of the (desired) impulse response $h^I_{\mathbf{H}}(t,\tau)$ whereas it is really an estimate of the output delay spread function $h^O_{\mathbf{H}}(t,\tau)$. This corresponds to a *misinterpretation error*

$$e_4(t,\tau) \triangleq h^O_{\mathbf{H}}(t,\tau) - h^I_{\mathbf{H}}(t,\tau). \tag{15}$$

  The effect of misinterpretation can be avoided by converting $\hat{h}^O_{\mathbf{H}}(t,\tau)$ into $\hat{h}^I_{\mathbf{H}}(t,\tau)$ via (1), i.e., $\hat{h}^I_{\mathbf{H}}(t,\tau) = \hat{h}^O_{\mathbf{H}}(t-\tau,\tau)$.

The error affecting the estimation of the time-varying frequency response $L^I_{\mathbf{H}}(t,f)$ can be split up similarly,

$$\hat{L}^O_{\mathbf{H}}(t,f) - L^I_{\mathbf{H}}(t,f) = \sum_{i=1}^{4} L_{e_i}(t,f),$$

where $L_{e_i}(t,f) \triangleq \mathcal{F}_{\tau\to f}\{e_i(t,\tau)\}$ (cf. (2)).

[4]The parameter K applies to the STDCC only. For other sounders, $K = 1$.

In the following, we shall present upper bounds on the error components $e_i(t,\tau)$ that are formulated in terms of channel and sounder parameters.

4.1 Aliasing Error

We first consider the aliasing error $e_3(t,\tau)$ in (14). This, in fact, is the aliasing error of the *idealized* channel sounder for which $\hat{h}^{O,\text{ideal}}_{\mathbf{H}}(t,\tau) = (\Upsilon\mathbf{H}\Delta_T)(t,\tau)$ (cf. (7)).

It can be shown [10] that for $\tau_{\max} \le T \le 1/(2K\nu_{\max})$ (which presupposes the underspread property $\tau_{\max}\nu_{\max} \le 1/(2K)$), subsequent snapshots do not overlap and the repetition rate is large enough so that $h^O_{\mathbf{H}}(t,\tau)$ is perfectly recovered after interpolation, i.e., $\hat{h}^{O,\text{ideal}}_{\mathbf{H}}(t,\tau) = h^O_{\mathbf{H}}(t,\tau)$. Otherwise, aliasing errors will occur since for $\tau_{\max} > T$ subsequent channel snapshots overlap and for $T > 1/(2K\nu_{\max})$ the sampling (repetition) rate is too small to track the channel's time variation. The aliasing error $e_3(t,\tau)$ can be shown [16] to be bounded as

$$\begin{aligned} \frac{\int_\tau |e_3(t,\tau)|\,d\tau}{\|S_{\mathbf{H}}\|_1} &\le \varepsilon_3^{(1)} \triangleq 2\left[\frac{\overline{\tau}^{(1)}_{\mathbf{H}}}{T} + 2KT\,\overline{\nu}^{(1)}_{\mathbf{H}}\right], \\ \frac{\|e_3\|_2}{\|S_{\mathbf{H}}\|_2} &\le \varepsilon_3^{(2)} \triangleq 2\left[\frac{\overline{\tau}^{(2)}_{\mathbf{H}}}{T} + 2KT\,\overline{\nu}^{(2)}_{\mathbf{H}}\right], \end{aligned} \tag{16}$$

with $\overline{\tau}^{(i)}_{\mathbf{H}}$, $\overline{\nu}^{(i)}_{\mathbf{H}}$, $i = 1,2$, as defined in Section 2. Similarly, $L_{e_3}(t,f) \triangleq \mathcal{F}_{\tau\to f}\{e_3(t,\tau)\}$ is bounded as

$$\frac{|L_{e_3}(t,f)|}{\|S_{\mathbf{H}}\|_1} \le \varepsilon_3^{(1)}, \qquad \frac{\|L_{e_3}\|_2}{\|S_{\mathbf{H}}\|_2} \le \varepsilon_3^{(2)}.$$

The bounds $\varepsilon_3^{(i)}$, $i = 1,2$, are minimized by choosing the sounding period T as $T^{(i)}_{\text{opt}} = \left[\overline{\tau}^{(i)}_{\mathbf{H}}/(2K\,\overline{\nu}^{(i)}_{\mathbf{H}})\right]^{1/2}$, in which case the minimum bounds are determined by $K\overline{\tau}^{(i)}_{\mathbf{H}}\overline{\nu}^{(i)}_{\mathbf{H}}$ [16]. Hence, for underspread channels (for which $\overline{\tau}^{(i)}_{\mathbf{H}}\overline{\nu}^{(i)}_{\mathbf{H}}$ will be small) and appropriately chosen sounding period T, the aliasing errors will be negligible.

4.2 Commutation Error

Next, we consider the commutation error $e_1(t,\tau)$ in (12). Adapting results from [8, 9], one can show the bound

$$\frac{|e_1(mT,\tau)|}{A\,\|S_{\mathbf{H}}\|_1\|r\|_1} \le \varepsilon_1^{(1)} \triangleq 2\pi\,\overline{\tau}_{\mathbf{R}}\,\overline{\nu}^{(1)}_{\mathbf{H}}, \tag{17}$$

where A is the maximum amplitude of the sounding signal $x(t) = (\mathbf{C}\Delta_T)(t)$ and $\overline{\tau}_{\mathbf{R}} \triangleq \int_\tau |\tau|\,|r(\tau)|\,d\tau/\|r\|_1$ is the effective duration of the receive filter impulse response $r(t)$. The above bound implies

$$\frac{\int_\tau |e_1(mT,\tau)|\,d\tau}{A\,\|S_{\mathbf{H}}\|_1\|r\|_1} \le T\varepsilon_1^{(1)}.$$

For typical receive filters for which $|r(t)|$ is constant within the interval $[0,T]$ and zero elsewhere, one obtains $\overline{\tau}_{\mathbf{R}} = T/2$. Hence, the above bounds imply that $e_1(mT,\tau)$ will be small if the product of the mean Doppler shift $\overline{\nu}^{(1)}_{\mathbf{H}}$ and the receive filter length T is small. For sounding period $T^{(1)}_{\text{opt}} = \left[\overline{\tau}^{(1)}_{\mathbf{H}}/(2K\,\overline{\nu}^{(1)}_{\mathbf{H}})\right]^{1/2}$, the bound $\varepsilon_1^{(1)}$, like the aliasing error bound $\varepsilon_3^{(1)}$, is effectively determined by $K\overline{\tau}^{(1)}_{\mathbf{H}}\overline{\nu}^{(1)}_{\mathbf{H}}$, and it will thus be small for underspread channels.

Ignoring aliasing errors in sounding the composite channel $\mathbf{RHC}$, i.e., assuming that $\hat{h}^O_{\mathbf{H}}(t,\tau) = h^O_{\mathbf{RHC}}(t,\tau)$ or equivalently $\hat{L}^O_{\mathbf{H}}(t,f) = L^O_{\mathbf{RHC}}(t,f)$, and using results

from [9], the following additional bounds can be shown,

$$\frac{\int_\tau |e_1(t,\tau)|\,d\tau}{\|c\|_1\|S_{\mathbf{H}}\|_1\|r\|_1} \le \tilde{\varepsilon}_1^{(1)} \triangleq 4\pi\left[\overline{\mu}_{\mathbf{RH}}^{(1)} + \overline{\mu}_{\mathbf{H}}^{(1)}\right],$$

$$\frac{\|e_1\|_2}{\|c\|_1\|S_{\mathbf{H}}\|_2\|r\|_1} \le \tilde{\varepsilon}_1^{(2)} \triangleq 4\pi\left[\overline{\mu}_{\mathbf{RH}}^{(2)} + \overline{\mu}_{\mathbf{H}}^{(2)}\right].$$

Similarly, $L_{e_1}(t,f) = \hat{L}_{\mathbf{H}}^{O}(t,f) - L_{\mathbf{HRC}}^{O}(t,f)$ is bounded as

$$\frac{|L_{e_1}(t,f)|}{\|c\|_1\|S_{\mathbf{H}}\|_1\|r\|_1} \le \tilde{\varepsilon}_1^{(1)}, \qquad \frac{\|L_{e_2}\|_2}{\|c\|_1\|S_{\mathbf{H}}\|_2\|r\|_1} \le \tilde{\varepsilon}_1^{(2)}.$$

The bound $\tilde{\varepsilon}_1^{(1)}$ can be simplified by using the inequality $\overline{\mu}_{\mathbf{RH}}^{(1)} \le \overline{\mu}_{\mathbf{H}}^{(1)} + \overline{\tau}_{\mathbf{R}}\overline{\nu}_{\mathbf{H}}^{(1)}$.

4.3 Pulse Compression Error

The pulse compression error $e_2(t,\tau)$ in (13) is due to $(c * r)(t) \neq \delta(t)$ or equivalently $C(f)R(f) \neq 1$. Let $D(f) = C(f)R(f) - 1$ denote the deviation of $C(f)R(f)$ from the ideal value 1. Again neglecting aliasing errors[5], one obtains

$$\frac{|e_2(mT,\tau)|}{\|S_{\mathbf{H}}\|_1} \le \|D\|_1, \qquad \frac{\|e_2\|_2}{\|S_{\mathbf{H}}\|_2} \le \|D\|_2, \quad (18)$$

$$\frac{|L_{e_2}(mT,f)|}{\|S_{\mathbf{H}}\|_1} \le |D(f)|, \qquad \frac{\|L_{e_2}\|_2}{\|S_{\mathbf{H}}\|_2} \le \|D\|_2.$$

4.4 Misinterpretation Error

Finally, the misinterpretation error in (15), $e_4(t,\tau) = h_{\mathbf{H}}^{O}(t,\tau) - h_{\mathbf{H}}^{I}(t,\tau)$, can be shown to be bounded as

$$\frac{\int_\tau |e_4(t,\tau)|\,d\tau}{\|S_{\mathbf{H}}\|_1} \le 2\pi\,\overline{\mu}_{\mathbf{H}}^{(1)}, \qquad \frac{\|e_4\|_2}{\|S_{\mathbf{H}}\|_2} \le 2\pi\,\overline{\mu}_{\mathbf{H}}^{(2)}. \quad (19)$$

Furthermore, in [9] it was shown that $L_{e_4}(t,f) = L_{\mathbf{H}}^{O}(t,f) - L_{\mathbf{H}}^{I}(t,f)$ is bounded as

$$\frac{|L_{e_4}(t,f)|}{\|S_{\mathbf{H}}\|_1} \le 2\pi\,\overline{\mu}_{\mathbf{H}}^{(1)}, \qquad \frac{\|L_{e_4}\|_2}{\|S_{\mathbf{H}}\|_2} \le 2\pi\,\overline{\mu}_{\mathbf{H}}^{(2)}.$$

Thus, for underspread channels where the moments $\overline{\mu}_{\mathbf{H}}^{(i)}$ are small, the misinterpretation error will be small, too.

5 CALIBRATION

Calibration aims at compensating for non-ideal pulse compression, i.e., $C(f)R(f) \neq 1$. Usually, the composite transfer function $C(f)R(f)$ of the transmit and receive filters is determined by a back-to-back measurement and a calibrated estimate of $L_{\mathbf{H}}^{O}(t,f)$ is then computed as

$$\widetilde{L}_{\mathbf{H}}^{O}(mT,f) \triangleq \frac{\hat{L}_{\mathbf{H}}^{O}(mT,f)}{C(f)R(f)}, \quad (20)$$

with $\hat{L}_{\mathbf{H}}^{O}(mT,f)$ as defined in (9). A calibrated estimate of $h_{\mathbf{H}}^{O}(mT,\tau)$ can then be obtained as $\widetilde{h}_{\mathbf{H}}^{O}(mT,\tau) = \mathcal{F}_{f\to\tau}^{-1}\{\widetilde{L}_{\mathbf{H}}^{O}(mT,f)\}$.

Unfortunately, whereas (20) yields perfect calibration in the case of time-invariant channels, for time-varying channels this is not true since here

$$L_{\mathbf{RHC}}^{O}(t,f) \neq C(f)\,L_{\mathbf{H}}^{O}(t,f)\,R(f).$$

The resulting systematic *calibration error* will be analyzed next. Furthermore, an improved calibration procedure will be proposed in Subsection 5.2.

[5] See [16] for bounds that take aliasing errors into account.

5.1 Calibration Error

Assuming calibration according to (20), and again disregarding aliasing errors for simplicity (i.e., assuming $\hat{L}_{\mathbf{H}}^{O}(t,f) = L_{\mathbf{RHC}}^{O}(t,f)$), the total systematic measurement error can be split into two contributions,

$$\widetilde{h}_{\mathbf{H}}^{O}(t,\tau) - h_{\mathbf{H}}^{I}(t,\tau) = e_4(t,\tau) + e_5(t,\tau).$$

Here, $e_4(t,\tau) = h_{\mathbf{H}}^{O}(t,\tau) - h_{\mathbf{H}}^{I}(t,\tau)$ is the misinterpretation error discussed in Section 4 and

$$e_5(t,\tau) \triangleq \widetilde{h}_{\mathbf{H}}^{O}(t,\tau) - h_{\mathbf{H}}^{O}(t,\tau)$$

is the *calibration error*. Using results from [9], one can show that the calibration error is bounded as[6]

$$\frac{\int_\tau |e_5(t,\tau)|\,d\tau}{\|S_{\mathbf{H}}\|_1} \le \varepsilon_5^{(1)} \triangleq 4\pi\left[\frac{\|c\|_1}{C_{\min}}\,\overline{\mu}_{\mathbf{HC}}^{(1)} + \overline{\mu}_{\mathbf{H}}^{(1)}\right], \quad (21)$$

$$\frac{\|e_5\|_2}{\|S_{\mathbf{H}}\|_2} \le \varepsilon_5^{(2)} \triangleq 4\pi\left[\frac{\|c\|_1}{C_{\min}}\,\overline{\mu}_{\mathbf{HC}}^{(2)} + \overline{\mu}_{\mathbf{H}}^{(2)}\right], \quad (22)$$

where $C_{\min}$ is the minimum of $|C(f)|$ over the signal band. Similarly, $L_{e_5}(mT,f) = \widetilde{L}_{\mathbf{H}}^{O}(mT,f) - L_{\mathbf{H}}^{O}(mT,f)$ is bounded as

$$\frac{|L_{e_5}(mT,f)|}{\|S_{\mathbf{H}}\|_1} \le \varepsilon_5^{(1)}, \qquad \frac{\|L_{e_5}\|_2}{\|S_{\mathbf{H}}\|_2} \le \varepsilon_5^{(2)}. \quad (23)$$

Since $\overline{\mu}_{\mathbf{HC}}^{(1)} \le \overline{\mu}_{\mathbf{H}}^{(1)} + \overline{\tau}_{\mathbf{C}}\overline{\nu}_{\mathbf{H}}^{(1)}$, an upper bound on $\varepsilon_5^{(1)}$ is determined by $\|c\|_1/C_{\min}$, the channel's mean delay-Doppler product, $\overline{\mu}_{\mathbf{H}}^{(1)}$, and the product of the transmit filter's mean delay, $\overline{\tau}_{\mathbf{C}}$, and the channel's mean Doppler shift, $\overline{\nu}_{\mathbf{H}}^{(1)}$. Note further that $|C(f)| \le \|c\|_1$ and hence $C_{\max}/C_{\min} \le \|c\|_1/C_{\min}$, i.e., $\|c\|_1/C_{\min}$ is an upper bound on the spectral flatness parameter $C_{\max}/C_{\min}$. Hence, poorly designed (non-flat) transmit filters must be expected to yield large calibration errors.

5.2 Improved Calibration

We now present a new calibration method that improves on the conventional calibration in (20). The new method is based on the following observations:

- The frequency responses of the actual transmit and receive filters can be written as $C(f) = C_0(f)C_d(f)$ and $R(f) = R_0(f)R_d(f)$, respectively, where $C_0(f)$ and $R_0(f)$ denote the *known* frequency responses of the nominal filters (e.g., PN sequence or chirp filter) and the *unknown* frequency responses $C_d(f)$ and $R_d(f)$ correspond to parasitic deviations from the nominal filters. Note that $\mathbf{RHC} = \mathbf{R}_0\mathbf{R}_d\mathbf{H}\mathbf{C}_d\mathbf{C}_0$.
- The frequency-dependent modulation function of the operator $\mathbf{R}_0\mathbf{H}'$, where $\mathbf{R}_0$ is a time-invariant system and $\mathbf{H}'$ is arbitrary, can be factored as [9]

$$L_{\mathbf{R}_0\mathbf{H}'}^{O}(t,f) = L_{\mathbf{H}'}^{O}(t,f)\,R_0(f). \quad (24)$$

- The time-varying frequency response of the operator $\mathbf{H}'\mathbf{C}_0$, where $\mathbf{H}'$ is arbitrary and $\mathbf{C}_0$ is a time-invariant system, can be factored as [9]

$$L_{\mathbf{H}'\mathbf{C}_0}^{I}(t,f) = C_0(f)\,L_{\mathbf{H}'}^{I}(t,f). \quad (25)$$

The new calibration/measurement method then consists of the following steps:

[6] The following bounds do not depend on $\mathbf{R}$ since, as will be stated in (24), the division by $R(f)$ in (20) is exact; only the division by $C(f)$ is an approximation.

1. Determine $C(f)R(f) = C_0(f)C_d(f)R_0(f)R_d(f)$ by means of back-to-back measurement. Using the known $C_0(f)$ and $R_0(f)$, calculate the product of parasitic frequency responses as
$$C_d(f)R_d(f) = \frac{C(f)R(f)}{C_0(f)R_0(f)}.$$
2. Measure $\hat{L}^O_{\mathbf{H}}(t,f)$ by means of channel sounding. Assuming that there are no aliasing errors, we have $\hat{L}^O_{\mathbf{H}}(t,f) = L^O_{\mathbf{RHC}}(t,f) = L^O_{\mathbf{R}_0\mathbf{R}_d\mathbf{H}\mathbf{C}_d\mathbf{C}_0}(t,f)$.
3. Compute $L^O_{\mathbf{R}_d\mathbf{H}\mathbf{C}_d\mathbf{C}_0}(t,f)$ according to
$$L^O_{\mathbf{R}_d\mathbf{H}\mathbf{C}_d\mathbf{C}_0}(t,f) = \frac{L^O_{\mathbf{R}_0\mathbf{R}_d\mathbf{H}\mathbf{C}_d\mathbf{C}_0}(t,f)}{R_0(f)} = \frac{\hat{L}^O_{\mathbf{H}}(t,f)}{R_0(f)},$$
where we have used (24) with $\mathbf{H}' = \mathbf{R}_d\mathbf{H}\mathbf{C}_d\mathbf{C}_0$.
4. Convert $L^O_{\mathbf{R}_d\mathbf{H}\mathbf{C}_d\mathbf{C}_0}(t,f)$ into $L^I_{\mathbf{R}_d\mathbf{H}\mathbf{C}_d\mathbf{C}_0}(t,f)$ by in turn calculating[7] (cf. (1), (2))
$$h^O_{\mathbf{R}_d\mathbf{H}\mathbf{C}_d\mathbf{C}_0}(t,\tau) = \mathcal{F}^{-1}_{f\to\tau}\{L^O_{\mathbf{R}_d\mathbf{H}\mathbf{C}_d\mathbf{C}_0}(t,f)\},$$
$$h^I_{\mathbf{R}_d\mathbf{H}\mathbf{C}_d\mathbf{C}_0}(t,\tau) = h^O_{\mathbf{R}_d\mathbf{H}\mathbf{C}_d\mathbf{C}_0}(t-\tau,\tau),$$
$$L^I_{\mathbf{R}_d\mathbf{H}\mathbf{C}_d\mathbf{C}_0}(t,f) = \mathcal{F}_{\tau\to f}\{h^I_{\mathbf{R}_d\mathbf{H}\mathbf{C}_d\mathbf{C}_0}(t,\tau)\}.$$
5. Compute $L^I_{\mathbf{R}_d\mathbf{H}\mathbf{C}_d}(t,f)$ according to
$$L^I_{\mathbf{R}_d\mathbf{H}\mathbf{C}_d}(t,f) = \frac{L^I_{\mathbf{R}_d\mathbf{H}\mathbf{C}_d\mathbf{C}_0}(t,f)}{C_0(f)},$$
where we have used (25) with $\mathbf{H}' = \mathbf{R}_d\mathbf{H}\mathbf{C}_d$.
6. Using $R_d(f)C_d(f)$ from Step 1, compute
$$\widetilde{L}^I_{\mathbf{H}}(t,f) \triangleq \frac{L^I_{\mathbf{R}_d\mathbf{H}\mathbf{C}_d}(t,f)}{R_d(f)C_d(f)}. \quad (26)$$
If necessary, the time-varying impulse response can then be calculated as $\widetilde{h}^I_{\mathbf{H}}(t,\tau) = \mathcal{F}^{-1}_{f\to\tau}\{\widetilde{L}^I_{\mathbf{H}}(t,f)\}$.

Note that a misinterpretation error is avoided due to Step 4. We emphasize that all steps are exact except for the final calibration in (26) in which the division through $R_d(f)$ is an approximation. This approximation is formally similar to the approximative division through $C(f)$ in (20). However, since typically the (effective) duration of $r_d(t)$ is much smaller than that of $c(t)$ (recall that the nominal part $r_0(t)$ has already been removed in Step 3), the resulting error will be much smaller. For example, $c_0(t) = r_0(T-t)$ might be a PN sequence consisting of several hundred chip pulses whereas $r_d(t)$ models the deviation from the ideal rectangular chip pulse shape and thus its duration is in the order of just a single chip length. The approximation error associated to (26), $e_6(t,\tau) \triangleq \widetilde{h}^I_{\mathbf{H}}(t,\tau) - h^I_{\mathbf{H}}(t,\tau)$, is bounded as (cf. (21)-(23))
$$\frac{\int_\tau |e_6(t,\tau)|\,d\tau}{\|S_{\mathbf{H}}\|_1} \le \varepsilon_6^{(1)} \triangleq 4\pi\left[\frac{\|r_d\|_1}{R_{d,\min}}\overline{\mu}^{(1)}_{\mathbf{R}_d\mathbf{H}} + \overline{\mu}^{(1)}_{\mathbf{H}}\right],$$
$$\frac{\|e_6\|_2}{\|S_{\mathbf{H}}\|_2} \le \varepsilon_6^{(2)} \triangleq 4\pi\left[\frac{\|r_d\|_1}{R_{d,\min}}\overline{\mu}^{(2)}_{\mathbf{R}_d\mathbf{H}} + \overline{\mu}^{(2)}_{\mathbf{H}}\right],$$
$$\frac{|L_{e_6}(mT,f)|}{\|S_{\mathbf{H}}\|_1} \le \varepsilon_6^{(1)}, \qquad \frac{\|L_{e_6}\|_2}{\|S_{\mathbf{H}}\|_2} \le \varepsilon_6^{(2)},$$

[7] For underspread channels, it may be more efficient to implement this conversion via relation (4).

The bound $\varepsilon_6^{(1)}$ can be simplified by using the inequality $\overline{\mu}^{(1)}_{\mathbf{R}_d\mathbf{H}} \le \overline{\mu}^{(1)}_{\mathbf{H}} + \overline{\tau}_{\mathbf{R}_d}\overline{\nu}^{(1)}_{\mathbf{H}}$.

6 SIMULATION AND MEASUREMENT RESULTS

We next present a numerical experiment to illustrate our theoretical results, and we demonstrate how our results can be used to assess the accuracy of measured data.

6.1 Simulation Results

We simulated the sounding of a channel consisting of a direct path with constant amplitude and a path with delay $\tau_{\max} = 10\,\mu$s and sinusoidally varying amplitude, i.e.,
$$h^I_{\mathbf{H}}(t,\tau) = a_0\,\delta(\tau) + a_1\cos(2\pi\nu_{\max}t)\,\delta(\tau-\tau_{\max}).$$
The carrier frequency was chosen as 1.8 GHz. The channel's Doppler frequency $\nu_{\max}$ was varied between 0.01 Hz and 370 Hz, corresponding to a velocity ranging from 0.006 km/h to 222 km/h. We assumed a correlation sounder using a PN sequence of length 127. With the sampling frequency chosen as 10 MHz, the duration of the PN sequence (= sounding period) is $T = 12,7\,\mu$s.

Without calibration, the relatively small length of the PN sequence caused the pulse compression error to dominate. The maximum pulse compression error $\frac{1}{\|S_{\mathbf{H}}\|_1}\max_{m,\tau}\{|e_2(mT,\tau)|\}$ and the corresponding upper bound $\|D\|_1$ in (18) were obtained as $7.9\cdot10^{-3}$ and $15.6\cdot10^{-3}$, respectively, for all values of $\nu_{\max}$. The maximum commutation error $\frac{1}{A\,\|S_{\mathbf{H}}\|_1\|r\|_1}\max_{m,\tau}\{|e_1(mT,\tau)|\}$ and the corresponding upper bound $\varepsilon_1^{(1)}$ in (17) are shown in Fig. 2(a) as a function of the Doppler frequency $\nu_{\max}$. Similarly, the maximum misinterpretation error $\frac{1}{\|S_{\mathbf{H}}\|_1}\max_m\{\int_\tau|\epsilon_4(mT,\tau)|\,d\tau\}$ and the corresponding upper bound $2\pi\overline{\mu}^{(1)}_{\mathbf{H}}$ in (19) are shown in Fig. 2(b). It is seen that both errors and the corresponding upper bounds grow with increasing Doppler frequency. The aliasing error is zero since with $\tau_{\max} = 10\,\mu$s, $\nu_{\max} \le 370$ Hz, and $T = 12,7\,\mu$s it follows that $\tau_{\max} \le T \le 1/(2\nu_{\max})$.

For the calibrated sounder using conventional calibration, the calibration error $\frac{1}{\|S_{\mathbf{H}}\|_1}\max_m\{\int_\tau|e_5(mT,\tau)|\,d\tau\}$ and the corresponding error bound $\varepsilon_5^{(1)}$ in (21) are shown in Fig. 2(c). Note that in our idealized example where the transmit and receive filters are completely known, the improved calibration presented in Section 5.2 would yield the channel impulse response without any error.

6.2 Evaluation of Measurements

In order to demonstrate how our error bounds can be used to assess the accuracy of existing measurements, we considered measurement results obtained with a RUSK XL channel sounder [17]. The carrier frequency is 1.8 GHz. The sampling frequency is 10 MHz, corresponding to a resolution of 0.1 μs. The impulse response snapshots consist of 1024 samples (corresponding to 102.4 μs, which is also the length of the transmit and receive filters). They were recorded every $T_{\text{rep}} = 49.152$ ms while the vehicle moved with an average velocity of 5.9 km/h (corresponding to a Doppler frequency of 9.83 Hz) through a typical suburban environment.

The measured data were used to estimate the following channel parameters: $\overline{\tau}^{(1)}_{\mathbf{H}} = 1.78\,\mu$s, $\overline{\nu}^{(1)}_{\mathbf{H}} = 6.49$ Hz, and $\overline{\mu}^{(1)}_{\mathbf{H}} = 1.11\cdot10^{-5}$. With these channel parameters and the sounder parameters given further above, we obtained

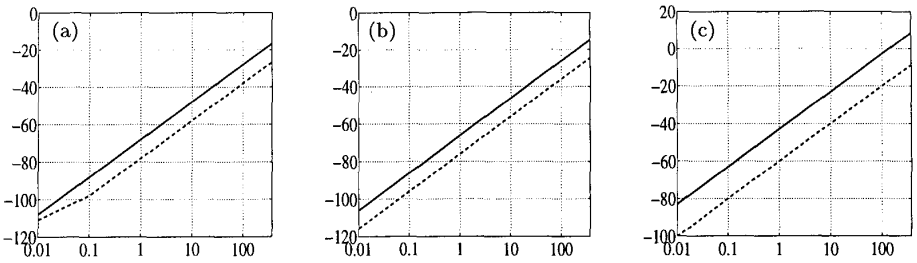

Figure 2. *Systematic measurement errors (dashed lines) and corresponding upper bounds (solid lines) in dB for a synthetic two-path channel: (a) Commutation error of uncalibrated sounder, (b) misinterpretation error of uncalibrated sounder, (c) calibration error of sounder using conventional calibration. The horizontal axis shows the Doppler frequency $\nu_{\max}$ in Hz.*

the upper bounds $\varepsilon_1^{(1)} = 2.1 \cdot 10^{-3}$ (commutation error), $\|D\|_1 = 9.76 \cdot 10^{-4}$ (pulse compression error), $\varepsilon_3^{(1)} = 1.28$ (aliasing error), $2\pi\,\overline{\mu}_{\mathbf{H}}^{(1)} = 7{\cdot}10^{-5}$ (misinterpretation error), and $\varepsilon_5^{(1)} = 4.5 \cdot 10^{-3}$ (calibration error). The large bound $\varepsilon_3^{(1)}$ suggests large aliasing errors. Since $\overline{\tau}_{\mathbf{H}}^{(1)} \ll T_{\text{rep}}$, these aliasing errors cannot be due to an overlap of successive snapshots; hence, they must be due to the repetition rate of $1/T_{\text{rep}}$ being too small to properly track the channel's time variations. This is in accordance with the fact that the repetition rate $1/T_{\text{rep}} = 20.35\,\text{Hz}$ is quite close to twice the average Doppler frequency $2\overline{\nu}_{\mathbf{H}}^{(1)} \approx 12.98\,\text{Hz}$. Moreover, the corresponding aliasing effects were clearly visible in the measured Doppler profile. The bounds $\varepsilon_1^{(1)}$ and $\varepsilon_5^{(1)}$ suggest that the commutation and calibration errors may be comparatively large (although still tolerable), which can be explained by the relatively long transmit and receive filters. Finally, the bound $2\pi\,\overline{\mu}_{\mathbf{H}}^{(1)}$ indicates that the misinterpretation error is negligible.

7 SUMMARY AND CONCLUSIONS

We have considered the correlative sounding of time-varying mobile radio channels. Based on a unifying, coherent mathematical framework for popular channel sounders we identified several distinct types of systematic measurement errors. We presented upper bounds on these measurement errors for both the uncalibrated and calibrated cases. These error bounds are formulated in terms of channel and sounder parameters, and they show that the systematic measurement errors will be small if the channel is underspread and if the transmit and receive filters are designed properly. We also presented a novel calibration technique that yields substantially improved calibration/estimation accuracy at the expense of increased computational costs (as compared to conventional calibration). We illustrated our theoretical results by numerical simulations and we demonstrated their usefulness in assessing the accuracy of measured channel data.

Acknowledgment. We thank Prof. Ernst Bonek for his support and encouragement as well as for critical reading of this manuscript.

REFERENCES

[1] J. D. Parsons, D. A. Demery, and A. M. D. Turkmani, "Sounding techniques for wideband mobile radio channels: A review," *IEE Proceedings-I*, vol. 138, pp. 437–446, Oct. 1991.

[2] P. J. Cullen, P. C. Fannin, and A. Molina, "Wide-band measurement and analysis techniques for the mobile radio channel," *IEEE Trans. Vehicular Technology*, vol. 42, pp. 589–603, Nov. 1993.

[3] P. C. Fannin, A. Molina, S. S. Swords, and P. J. Cullen, "Digital signal processing techniques applied to mobile radio channel sounding," *IEE Proceedings-F*, vol. 138, pp. 502–508, Oct. 1991.

[4] P. A. Bello, "Characterization of randomly time-variant linear channels," *IEEE Trans. Comm. Syst.*, vol. 11, pp. 360–393, 1963.

[5] W. Kozek, "On the generalized Weyl correspondence and its application to time-frequency analysis of linear time-varying systems," in *Proc. IEEE-SP Int. Sympos. Time-Frequency Time-Scale Analysis*, (Victoria, Canada), pp. 167–170, Oct. 1992.

[6] R. S. Kennedy, *Fading Dispersive Communication Channels*. New York: Wiley, 1969.

[7] H. L. Van Trees, *Detection, Estimation, and Modulation Theory, Part III: Radar-Sonar Signal Processing and Gaussian Signals in Noise*. Malabar (FL): Krieger, 1992.

[8] W. Kozek, "On the transfer function calculus for underspread LTV channels," *IEEE Trans. Signal Processing*, vol. 45, pp. 219–223, Jan. 1997.

[9] G. Matz and F. Hlawatsch, "Time-frequency transfer function calculus (symbolic calculus) of linear time-varying systems (linear operators) based on a generalized underspread theory," *J. Math. Phys.*, vol. 39, pp. 4041–4071, Aug. 1998.

[10] T. Kailath, "Measurements on time-variant communication channels," *IEEE Trans. Inf. Theory*, vol. 8, pp. 229–236, Sept. 1962.

[11] T. Felhauer, P. Baier, W. König, and W. Mohr, "Optimum spread spectrum signals for wideband channel sounding," *Electronic Letters*, vol. 29, pp. 563–564, March 18th 1993.

[12] A. Molina and P. C. Fannin, "Application of mismatched filter theory to bandpass impulse response measurements," *Electronic Letters*, vol. 29, pp. 162–163, January 21st 1993.

[13] D. Cox, "Delay Doppler characteristics of multipath propagation in a suburban mobile radio environment," *IEEE Trans. Antennas and Propagation*, vol. 20, pp. 625–635, 1972.

[14] S. Salous, N. Nikandrou, and N. Bajj, "Digital techniques for mobile radio chirp sounders," *IEE Proc. Commun.*, vol. 145, pp. 191–196, June 1998.

[15] M. Skolnik, *Radar Handbook*. New York: McGraw-Hill, 1984.

[16] A. F. Molisch, G. Matz, M. Steinbauer, F. Hlawatsch, I. Gaspard, and H. Artés, "Systematic errors of mobile radio channel measurements with correlation sounders." To be submitted.

[17] K. Schwarz, U. Martin, and H. W. Schüßler, "Devices for propagation measurements in mobile radio channels," in *Proc. IEEE PIMRC-93*, pp. 387–391, 1993.